

Sonophotocatalytic degradation of sodium diclofenac using low power ultrasound and micro sized TiO₂

Daniela Meroni^{1,+}, Marta Jiménez-Salcedo^{2,+}, Ermelinda Falletta¹, Bianca M. Bresolin³, Chong Fai Kait⁴, Daria C. Boffito⁵, Claudia L. Bianchi¹, Carlo Pirola^{1,*}

¹ *Università degli Studi di Milano, Dipartimento di Chimica, via Golgi, 19 – 20133 Milano (Italy)*

² *University of La Rioja, Centro de Investigación en Síntesis Química (CISQ), Department of Chemistry, C/Madre de Dios 51, E-26006 Logroño La Rioja (Spain)*

³ *Lappeenranta University of Technology, Laboratory of Green Chemistry, School of Engineering Science, Sammonkatu 12 -50130, Mikkeli (Finland)*

⁴ *Universiti Teknologi PETRONAS, Fundamental & Applied Sciences Department – 32610 Seri Iskandar (Malaysia)*

⁵ *Polytechnique Montréal – Génie Chimique 2900 Boul. Edouard Montpetit – H3T 1J4 Montréal, QC (Canada)*

* *Corresponding Author: carlo.pirola@unimi.it*

+ *These authors contributed equally*

Abstract

The nonsteroidal anti-inflammatory drug sodium diclofenac (DC) is an emerging water pollutant which resists conventional wastewater treatments. Here the sonophotocatalytic degradation of DC was carried out using micrometric TiO₂ (both pristine and Ag-decorated), UV-A irradiation and 20 kHz pulsed ultrasound. Sonophotocatalytic tests were compared with photolysis, sonolysis, sonophotolysis, sonocatalysis and photocatalysis data performed in the same conditions. A synergy index of over 2 was determined for tests with pristine TiO₂, while values close to 1.3 were observed for Ag-TiO₂. Reaction intermediates were studied by HPLC-MS, showing degradation mechanisms activated by hydroxyl radicals. Similar pathways were identified for photocatalytic and sonophotocatalytic tests, although the latter led to more oxidized compounds. Different reactor configurations (static and dynamic set ups) were studied. Sequential and simultaneous application of UV light and ultrasound led to similar performance. The role of water matrix was investigated using ultrapure and drinking water, showing marked detrimental effects of electrolytes on the DC

degradation. Overall, the combined treatment proved more efficient than photocatalysis alone especially in demanding working conditions, like in drinking water matrices.

Keywords

Diclofenac; low power ultrasound; micro TiO₂; photocatalysis; persistent organic pollutants; water remediation

1. Introduction

The absence of guidelines and standards to detect numerous pharmaceuticals and personal care products (PPCPs) in wastewaters, surface and groundwater is causing increasing concerns [1]. The long-term effects of exposure to these compounds on human health and the environment are poorly understood [2]. Many of these molecules are recalcitrant to biodegradation and conventional wastewater treatments, leading to accumulation in the environment and bioaccumulation phenomena [3]. To address this problem several technologies have been considered, including sorption, biodegradation, photodegradation and oxidation technologies [4]. Adsorption on solids, such as activated carbon, can be used for the removal of numerous micropollutants in wastewater treatment plants (WWTPs) [5], but require the periodic regeneration of the adsorbent and simply transfer pollutants from the liquid to a solid phase. Biodegradation can transform undesired organic compounds via reactions assisted by bacteria, algae, or fungi; nevertheless, the bacteria-assisted biodegradation of persistent pollutants is found to be rare under aerobic conditions [6], like those occurring in WWTPs. The degradation promoted by direct light (near UV and visible radiation) shows performance strongly dependent on the pollutant absorption spectrum and, consequently, is limited to specific compounds suitable to be activated by light [7]. Moreover, as only some specific bonds in the molecules can be broken by the direct action of light, complete degradation to non-toxic compounds is very difficult to attain. Oxidation processes are based on strong oxidizing agents such as hydroxyl radicals [8], ozone [9], chlorine [10] and potassium permanganate [11]. Advanced Oxidation Processes (AOPs) include a range of techniques that enhance the formation of free hydroxyl radicals, which can lead to the complete degradation of recalcitrant pollutants. Ozonation, heterogeneous photocatalysis with semiconductor solid particles, Fenton oxidation, and sonolysis are among the main AOP technologies, which can be used alone or in combination [12][13][14][15]. Combining has gained traction as it reduces the processing time and limits the formation of toxic intermediates [16] [17] [18].

In this context, ultrasound (US)-assisted photocatalysis represents a consolidated and largely investigated technique for water remediation [19] [20] [21]. The main advantage of this combined approach is the excellent performance in terms of pollutant degradation: cavitation can enhance the efficiency of photocatalysis by promoting mass transfer and by increasing the formation of radicals, which are the active species involved in degradation reactions [22] [23]. Moreover, in presence of US, the semiconductor surface is continuously regenerated *in situ* [24], potentially extending the photocatalyst lifetime. However, the occurrence of synergistic enhancements depends on several factors, including the nature of the pollutant (such as its volatility and hydrophilic/hydrophobic nature), the US frequency and power, and mass diffusion within the adopted reactor [25] [26] [27].

In order to evaluate the sustainability of the technology, it is crucial to consider not only the energy requirements and cost, but also its potential impact on the environment and public health [20]. Considering US-promoted photocatalysis, the energy required by US production and lamps for irradiation should be evaluated and referred to the amount of removed pollutant [12] [20]. Moreover, the nanometric size of commonly employed heterogeneous photocatalysts makes separation at the end of the remediation process a costly and lengthy procedure. In addition, the health and environmental effects of nanosized particles have come under increased scrutiny [28] [29]. In this regard, the use of micro-sized particles, titanium dioxide in particular, can represent a friendlier alternative. Bianchi *et al.* [30] reported similar performance of commercial nano (Evonik P25) and micro (Kronos 1077) TiO₂ particles in the photocatalyzed degradation of volatile organic compounds, opening a new pathway for the application of microparticles as heterogeneous photocatalysts.

Another important difference between laboratory studies and real application is the adopted water matrix. The preferential use in laboratory tests of ultrapure water neglects the effects of electrolytes and common contaminants on light transmission inside the reactor, as well as competitive interactions with the photocatalyst surface and with the active radicals [31] [32].

In the vast class of emerging water pollutants, diclofenac (DC), a synthetic non-steroidal anti-inflammatory drug (NSAD) largely used as analgesic [33], is causing growing concern due to the exponential growth in its usage, its inefficient removal by WWTPs (which causes almost 75% of the used DC to enter surface waters and soil [34]), and its environmental persistence related to its hydrophilicity and chemical stability [35]. Diclofenac and its metabolites have been shown to be ubiquitous in nearly all water and soil environmental compartments and the biota [35]. Moreover, diclofenac represents a challenging case study for US-assisted photocatalysis, as previous works have reported only a slight synergistic enhancement in the degradation of the parent compound accompanied by a detrimental effect on the overall mineralization [16] [36].

In this context, the present study focuses on the degradation of sodium diclofenac by US-assisted photocatalysis using low power, low frequency, pulsed sonication and microsized TiO₂ photocatalysts (both pristine and promoted with Ag). Different reactor configurations were considered along with the effect of water matrix, employing both ultrapure and drinking water. It should be noted that previous studies used conditions largely different with respect to those adopted in the present work, in particular for what concerns US parameters and TiO₂ particle size. Our results support substantial synergistic effects of DC removal using low frequency sonication. Moreover, the study of transformation products revealed a beneficial effect of the ultrasound-

assisted process on the DC degradation, especially when demanding tests conditions (like real water matrices) are employed.

2. Materials and Methods

Diclofenac sodium ($\geq 99\%$) was purchased from Sigma-Aldrich (Germany). HPLC-grade acetonitrile was provided by Fischer Scientific and formic acid (98%) by Sigma-Aldrich. Micrometric TiO_2 was used as photocatalyst: Kronos 1077, which is pure anatase TiO_2 with an average crystallite size of 110 nm, was used either in its pristine form (labeled as TiO_2 in this paper) or upon decoration with Ag nanoparticles (labeled as Ag- TiO_2 in the text) using a procedure previously reported [37] based on TiO_2 impregnation by electrochemically synthesized Ag nanoparticles, followed by calcination at 400 °C. A full characterization of both TiO_2 and Ag- TiO_2 has been previously reported [37].

Tests were carried out either in ultrapure water (doubly distilled water passed through a milliQ apparatus) or in drinking water from the Milan water supply network (sampled from September to December 2019); a representative drinking water composition is reported in Table 1.

Table 1. Main physicochemical parameters of tap water used in DC degradation tests (source: Metropolitane Milanesi)

parameter	average value
<i>pH</i>	7.6
<i>total dissolved solids</i>	376 mg L ⁻¹
<i>hardness</i>	30 °fH
<i>conductivity (at 20°C)</i>	579 μS cm ⁻¹
<i>Ca²⁺</i>	85 mg L ⁻¹
<i>Mg²⁺</i>	18.9 mg L ⁻¹
<i>Cl⁻</i>	33 mg L ⁻¹
<i>SO₄²⁻</i>	52 mg L ⁻¹
<i>Na⁺</i>	19 mg L ⁻¹
<i>HCO₃⁻</i>	223 mg L ⁻¹
<i>NO₃⁻</i>	30 mg L ⁻¹
<i>residual chlorine</i>	0.01 mg L ⁻¹

2.1 Degradation test setup and procedure

Degradation tests by sonolysis, photolysis, photocatalysis and US-assisted photocatalysis were performed using different experimental configurations, reported in Figure 1. Figure 1a shows a conventional batch setup where US and UV irradiation could be simultaneously performed. We will label as “static” the runs conducted using the configuration in Figure 1a. Alternatively, two separate reactors were employed and the reaction mixture was continuously recirculated from one reactor to the other by a pump: tests carried out with this configuration will be labeled as “dynamic” runs. When the sonication and light irradiation were performed in different reactors, the dynamic configuration will be named as “type I” (Figure 1b), whereas when the US horn was placed in the same reactor where UV irradiation took place, the dynamic setup will be called “type II” (Figure 1c).

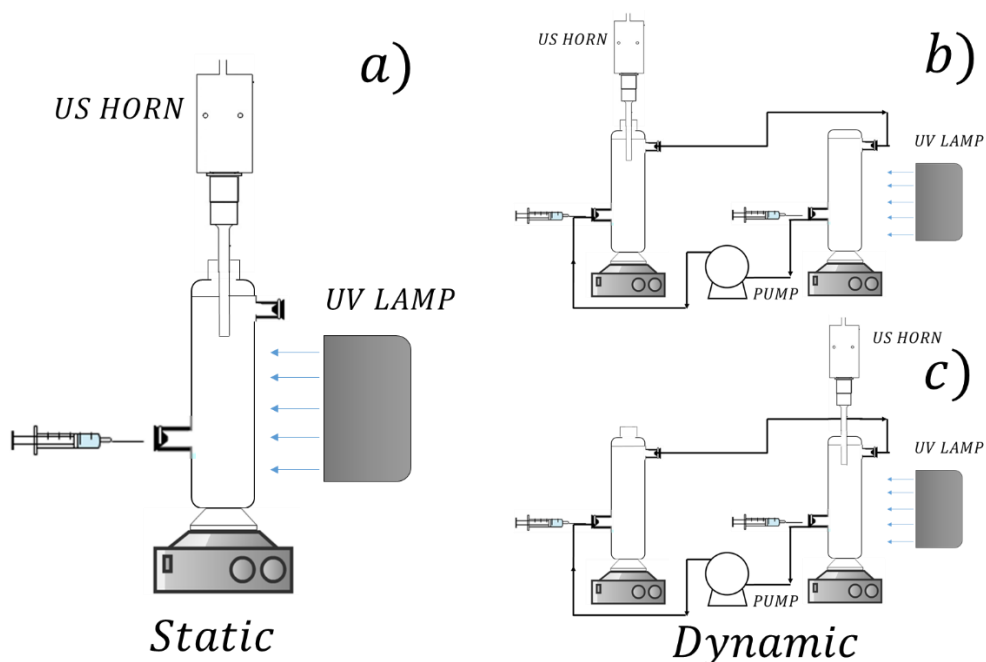


Figure 1. Experimental setups for DC degradation tests: static runs configuration (a), type I dynamic configuration (b) and type II dynamic configuration (c).

Degradation experiments were carried out at 45°C and spontaneous pH (initial value *ca.* 5.5). It should be noted that the average temperature of water inlet in wastewater plants is *ca.* 20 °C; however, the water temperature in wastewater plants can vary greatly, also depending on the type of applied treatment. In the case of photocatalytic plants, higher temperatures have been reported, sometimes even higher than 40 °C [38] [39]. As previous reports have highlighted a role of the reaction temperature on photocatalytic [40] and sonophotocatalytic [41] degradation of pollutants, with optimal temperature in the range 20-30 °C, we are here testing quite demanding reaction conditions which could however occur in WWTPs.

During all of the performed tests, a constant stirring was maintained via a magnetic stirrer. Magnetic stirring was required to ensure a sufficient mixing of the system to avoid diffusion limitations and to maintain the micrometric catalyst in suspension. Diffusion limitations were excluded by running experiments using different stirring rates which yielded comparable results. Reproducibility was evaluated by repeating each test twice.

A 0.1 g/L photocatalyst load was suspended either in 600 mL (static tests) or 2 L (dynamic tests) of a 25 ppm sodium diclofenac (DC) solution, prepared either in ultrapure or drinking water.

During photolysis, photocatalytic and sonophotocatalytic tests, light irradiation was provided by a UV-A lamp (halide lamp, 500 W, 320-400 nm, effective power density of irradiation 35 W m^{-2}).

During sonolysis and sonophotocatalytic tests, a 20 kHz ultrasonic processor (VibraCell VCX 500, Sonics and Materials) was placed on top of the reactor and the 136 mm-long US probe was immersed into the reaction liquid, avoiding contact with the reactor walls. A 13 mm-diameter titanium alloy (Ti-6Al-4 V) tip was used. Tests were carried out using pulsed sonication, adopting 5 s pulses separated by 5 s intervals. The effective US power was measured by calorimetric calibration, as discussed in Section 3.1.

For monitoring DC depletion and transformation products (TPs) during degradations, aliquots were withdrawn at time intervals, filtered (nylon $0.22 \mu\text{m}$) and analyzed by ultra-performance liquid chromatography (UPLC) using a Ultimate 3000 system (Thermo Fisher Scientific) equipped with an autosampler, temperature-controlled column compartment and UV detector as a chromatographic system that was interfaced with a Thermo Fisher LCQ Fleet ion trap mass spectrometer (MS) with an electrospray ionization source (ESI). The chromatographic separation of the organic mixtures was performed at 30°C and with a 0.25 mL/min flow, by injecting $20 \mu\text{L}$ samples. The separation column was a Zorbax RX-C18 ($2.1 \times 150 \text{ mm} - 5 \mu\text{m}$ column) and elution was carried out with a binary gradient consisting of $\text{H}_2\text{O} + 0.1\% \text{ HCOOH}$ (A) and $\text{CH}_3\text{CN} + 0.1\% \text{ HCOOH}$ (B). The gradient started from 30% B and increased to 50% B in 15 min. After 5 min (25 min) phase B reaches 60% and 100% at 25 min. Finally, the chromatographic system was reconditioned in 5 min. The MS interface conditions for sample acquisition were the following: heater temperature 150°C , sheath gas flow rate (arb) 20, auxiliary gas flow rate (arb) 10, sweep gas flow rate (arb) 10, spray voltage negative mode 3.50 kV, capillary temperature 275°C , capillary voltage -10 V, tube lens -10 V, m/z range 50–500 Da.

A toxicology assessment of the degradation intermediates was performed using the Toxtree software (v3.1.0.1851) according to Cramer rules with extensions.

3. Results and discussion

3.1 Ultrasound power calibration

The power of ultrasound released to the reacting media is a key parameter for US assisted reactions and processes. The reproducibility of experimental runs and the estimated energy consumption of the process are strongly dependent on this parameter. In order to take into account the energy efficiency of the used sonicator, power calibration is required for an accurate definition of the output power. Among the different calibration methods [42], the calorimetric approach is one of the easiest and most accurate [43]. In this work, the calibration of our 20 kHz US processor was performed according to a literature procedure [43], based on the temperature increase of a weighted amount of ultrapure water as a function of sonication time. Figure 2a reports the calibration curves for three different amplitudes (20, 30, 40%) and the resulting dependence of the US output power on the instrument amplitude is shown in Figure 2b.

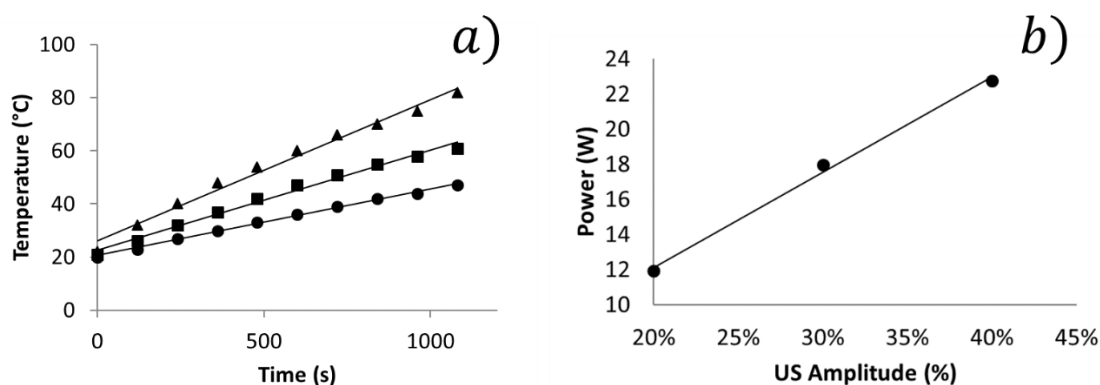


Figure 2. a) Calibration curves for three different amplitudes: 20 (circles), 30 (squares), and 40% (triangles); b) dependence of the US output power (W) on the instrument amplitude.

The power released by the ultrasound in the water results in a linear increase in the temperature of the calibration reactor (Fig. 2a). This trend is linear if the instrument is working in stationary conditions (i.e. a warm up period is required before the calibration) and if a small increase of temperature is considered [43]. The US power emitted from the horn, which differs from the power taken from the electric grid due to the instrument efficiency, increases by increasing the US amplitude of the instrument. US amplitude is an arbitrary unit of the sonicator, while the emitted power determined by calibration is an independent characteristic of the experimental setup. All of the DC degradation tests involving US irradiation were carried out using a 40% amplitude, hence a US output power of 23 W.

3.2 Static degradations of sodium diclofenac using Kronos TiO₂

DC degradation tests by different AOPs were carried out on the static setup: sonolysis (labeled as US), photolysis (UV), ultrasound-assisted photolysis (UV-US), photocatalysis (TiO₂-UV), sonolysis in the presence of the photocatalyst (TiO₂-US), and ultrasound-assisted photocatalysis (TiO₂-UV-US). The relative DC disappearance curves of tests in ultrapure and drinking water are reported in Figure 3a and 3b, respectively.

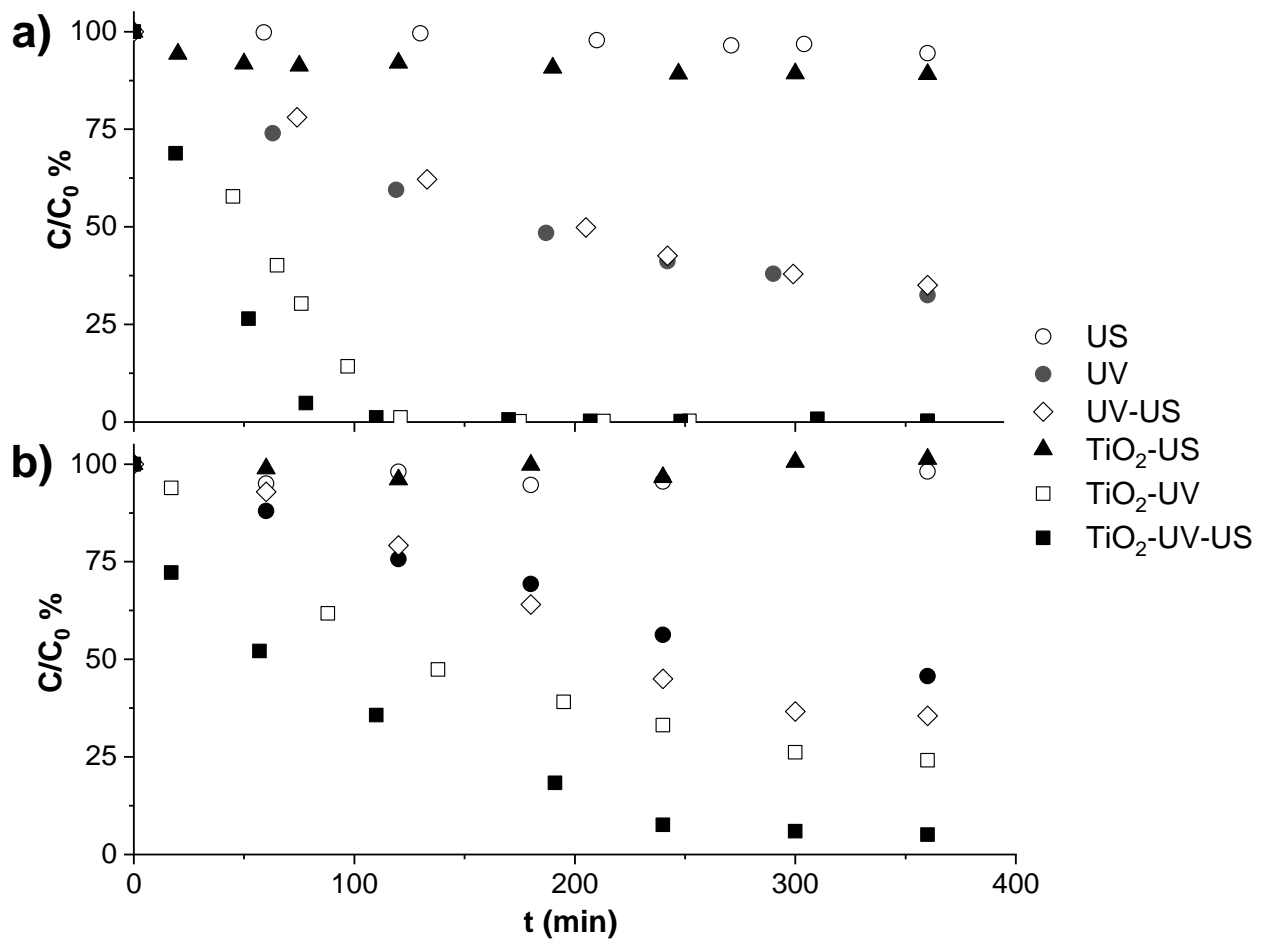


Figure 3. DC disappearance curves during degradation tests on a static setup in a) ultrapure water and b) drinking water; average standard deviation is 2% for tests in ultrapure water and 4% for tests in drinking water; $C_0 = 25$ ppm, 0.1 g/L of TiO₂ photocatalyst, 20 kHz and 23 W pulsed sonication.

All of the degradations follow a pseudo-first order kinetics. A summary of the kinetic data in ultrapure and drinking water is reported in Table 2. The synergy index of combined treatments was calculated according to the equations [22]:

$$\text{Synergy index (TiO}_2 - \text{UV} - \text{US)} = \frac{k(\text{TiO}_2 - \text{UV} - \text{US})}{k(\text{TiO}_2 - \text{UV}) + k(\text{TiO}_2 - \text{US})}$$

$$\text{Synergy index (UV - US)} = \frac{k(\text{UV} - \text{US})}{k(\text{UV}) + k(\text{US})}$$

Table 2. Pseudo-first order rate constants, k , the relative correlation coefficient of linear regression, and synergy index (where applicable) of DC degradation tests carried out in ultrapure and drinking water on a static setup.

degradation test	ultrapure water			drinking water		
	k ($\cdot 10^{-3} \text{ min}^{-1}$)	R^2	synergy index	k ($\cdot 10^{-3} \text{ min}^{-1}$)	R^2	synergy index
US	0.13 ± 0.01	0.939	-	0.24 ± 0.06	0.790	-
TiO ₂ -US	0.43 ± 0.07	0.824	-	0.13 ± 0.05	0.259	-
UV	3.4 ± 0.1	0.989	-	2.27 ± 0.08	0.995	-
UV-US	3.2 ± 0.1	0.994	0.91	2.2 ± 0.2	0.972	0.92
TiO ₂ -UV	15 ± 1	0.971	-	4.7 ± 0.1	0.996	-
TiO ₂ -UV-US	34 ± 3	0.980	2.20	9.7 ± 0.3	0.993	2.01
Ag-TiO ₂ -UV	33 ± 1	0.992	-	5.0 ± 0.1	0.997	-
Ag-TiO ₂ -UV-US	46 ± 1	0.996	1.38	6.4 ± 0.3	0.986	1.25

Figure 3 shows that the depletion of DC due to sonolysis (US) is almost negligible, irrespectively of the water matrix. This result can be rationalized considering the low US frequency here adopted (20 kHz), which leads to a low number of formed cavitation bubbles [44]. When sonication is carried out in the presence of the photocatalyst (TiO₂+US), DC degradation in ultrapure water shows a slight improvement. It should be noted that dark adsorption tests in both ultrapure and drinking water led to a negligible DC disappearance after 360 min. In the literature, mixed results have been reported on the effect of oxide addition during sonolytic degradation of diclofenac [16] [45]. Oxide micro-pores can act as cavitation nuclei [46], slightly promoting pollutant removal [45]. Conversely, other authors have reported detrimental effects of oxide addition, which were attributed to lower cavitation activity caused by acoustic waves scattering by solid particles [16]. In the present case, the slower build up of the main degradation intermediate (see Section 3.4) observed upon TiO₂ addition, along with the slight detrimental effect of TiO₂ on the DC removal rate constant in drinking water, seem to support a loss of cavitation activity ensuing the oxide supplementation.

Photolysis (UV) leads instead to a higher pollutant removal in both the considered water matrices, leading to over 50% DC disappearance after 360 min of irradiation. DC has been reported to be susceptible to photolysis, due to its light absorption in the UV-A region and relatively high quantum

yield [47] [48]. By comparing tests in ultrapure and drinking water, a detrimental effect of electrolytes and other contaminants is appreciable, resulting in a 10% decrease in the total DC disappearance. Previous studies about UV-A photolysis of DC in various water matrices have often shown a beneficial effect of complex matrices like wastewaters [49] [50], which is generally attributed to the presence of dissolved organic matter and nitrates acting as photosensitizers [51]. However, in the present study, our complex water matrix (drinking water) presents a low content of dissolved organic compounds, whereas the radical scavenging effect of inorganic anions (chlorides, carbonates, sulfates) appears to be prevalent [51]. Combining sonication to photolysis (UV-US) leads to a slight detrimental effect, as also testified by the synergy index < 1 .

The addition of the TiO_2 photocatalyst greatly promotes the DC disappearance, leading to a five-fold increase in the rate constant for photocatalytic tests (TiO_2 -UV) with respect to photolysis, in agreement with previous reports [52]. A complete disappearance of the parent compound is observed in about 120 min of irradiation. It is noteworthy that previous reports about photocatalytic degradation of DC using micrometric TiO_2 showed much lower performance, especially with respect to nanometric photocatalysts [53]. In the present case, competitive performance in terms of DC removal is observed using commercial micro TiO_2 .

As observed in photolysis tests, the use of a real water matrix markedly decreases DC degradation. The effect of the water matrix on photocatalytic activity is even more striking than in the case of photolysis tests: an almost 70% drop in the rate constants is observed when drinking water is used in photocatalytic tests, to be compared with a 30% decrease in photolysis runs. The detrimental role of inorganic salts on photocatalysis has been widely reported [32], also in the case of diclofenac degradation [51]. In particular, previous studies on the photocatalytic degradation of DC in different water matrices have shown almost comparable negative effects of largely different matrices such as wastewaters and drinking water [54] [53]. This observation supports a main negative role of electrolytes. Indeed, inorganic salts can block active sites at the photocatalyst surface, as well as compete for free radicals. Moreover, the increase in ionic strength can also induce agglomeration of the photocatalyst reducing the available surface area.

By combining sonication and photocatalysis (TiO_2 -UV-US), a further enhancement of the DC removal is here observed: the complete disappearance of the molecule is observed in *ca.* 80 min. By analyzing the rate constants, synergistic effects can be determined between the two combined AOPs. On the grounds of the rate constant values reported in Table 2, a synergy index of 2.20 was calculated for the DC disappearance in the ultrasound-assisted photocatalytic process using Kronos TiO_2 . This value compares favorably with literature studies on DC degradation by sonophotocatalytic processes: Bagal and Gogate reported a synergy index of 1.43 [36] using

hydrodynamic cavitation and nanometric anatase-rutile TiO₂, while Madhavan et al. reported a value of 1.3 [16] employing 213 kHz continuous sonication and P25 TiO₂ with a specific power in the range 15-55 mW/mL. Our experimental runs have been conducted using US with similar low specific power (0.038 mW/mL), but using a frequency largely lower (20 kHz). In this respect, it should be noted that previous reports highlighted a role of the sonication frequency on the synergy of sonophotocatalytic processes [44]. In particular, more marked synergistic effects were observed using low frequency sonication, as the one adopted in the present study.

The occurrence of synergistic effects in the degradation of DC by sonophotocatalysis has been mainly attributed to the multiple available pathways for H₂O₂ scission, produced either via photocatalysis or sonolysis [16], which can give rise to highly reactive hydroxyl radicals [44]. This hypothesis is supported, in the present case, by the identified reaction intermediates (see Section 3.4). The addition of electrolytes in the water matrix does not significantly alter the synergy index of the combined process, which remains higher than 2. It is noteworthy that, when the water matrix is changed, a 70% decrease in the rate constant of DC disappearance is observed for the combined process, similarly to what observed for the sole photocatalysis. This indicates that ultrasound-assisted processes do not interfere with the electrolyte-induced detrimental effects on the reaction kinetics.

3.2 *Dynamic set-ups*

The role of the experimental setup on the ultrasound-assisted process was investigated by comparing two different reactor configurations, where the UV irradiation and sonication treatment could be performed either simultaneously or sequentially. Tests were carried out using two reactors where the reaction mixture was recirculated continuously: UV and US treatment were performed in different reactors (type I) or in the same reactor (type II); in the latter setup, the second reactor was used only for recirculating the suspension. As a result, in both of the dynamic setups, each milliliter of suspension was subjected to light irradiation for less than half of the overall run time and analogously to sonication for less than half of the overall run time. Consequently, the observed DC removal rate are lower than for the static setup and direct comparisons can be made only between the two dynamic setups. Moreover, all the main operative parameters are different between static and dynamic tests. The size, shape and fluid-dynamic behavior of dynamic reactors are different. The propagation and the intensity of US and UV are totally modified too. For this reason, this study aims at comparing mainly the role of the UV and US source locations in dynamic configurations.

Figure 4 reports the DC disappearance curves of ultrasound-assisted photocatalytic tests performed using dynamic set-ups in both ultrapure and drinking water. As in the static degradations, the DC

depletion in ultrapure water is faster than in drinking water. Degradation curves of the two set-ups are fully comparable. This result demonstrates that the kinetic rate of the degradation reaction is not dependent on the used configuration. In other words, US and UV can be applied in the same site or in different points of the reactor without changing the degradation performance. Then, the active species do not require the simultaneous local presence of UV and US source action. This result is important for future scale up considerations of the technology.

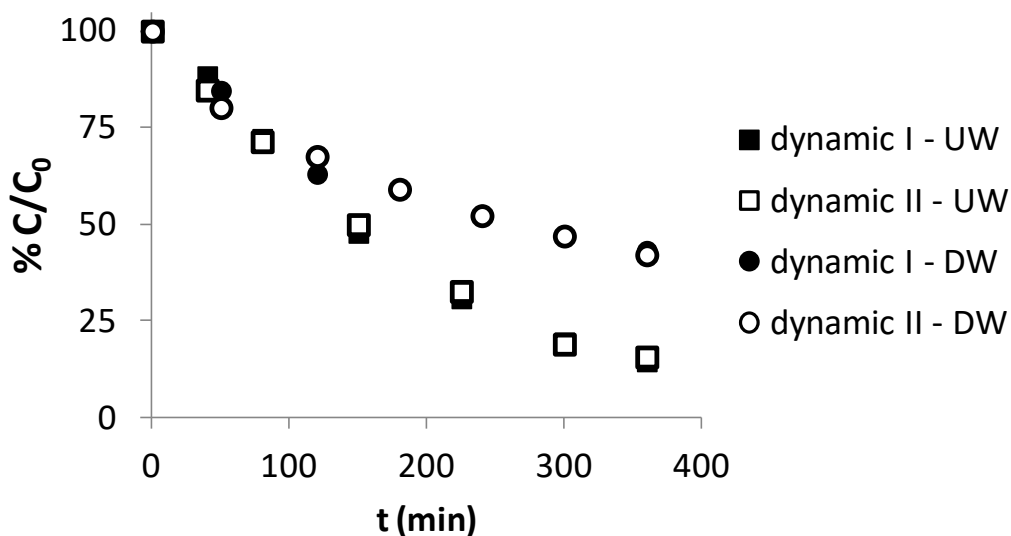


Figure 4 – DC disappearance during dynamic tests in ultrapure (UW) and drinking water (DW). The average estimated standard deviation is below 2%.

3.3 Static degradation tests of sodium diclofenac using Ag-decorated TiO₂

Promotion with noble metal nanoparticles is a strategy often adopted in photocatalysis to enhance the performance due to plasmonic effects and charge carrier dynamics [55]. Some of us have recently reported highly beneficial effects of the promotion of micrometric TiO₂ with Ag colloidal particles towards the gas-phase degradation of acetone [56]. In the present study, we compared the photocatalytic and sonophotocatalytic activity of pristine and Ag-promoted micro TiO₂ towards the degradation of DC. Figure 5 compares the DC removal curves of both catalysts in photocatalytic and ultrasound-assisted tests in ultrapure and drinking water. The relative kinetics data are reported in Table 2, along with the calculated synergy indexes.

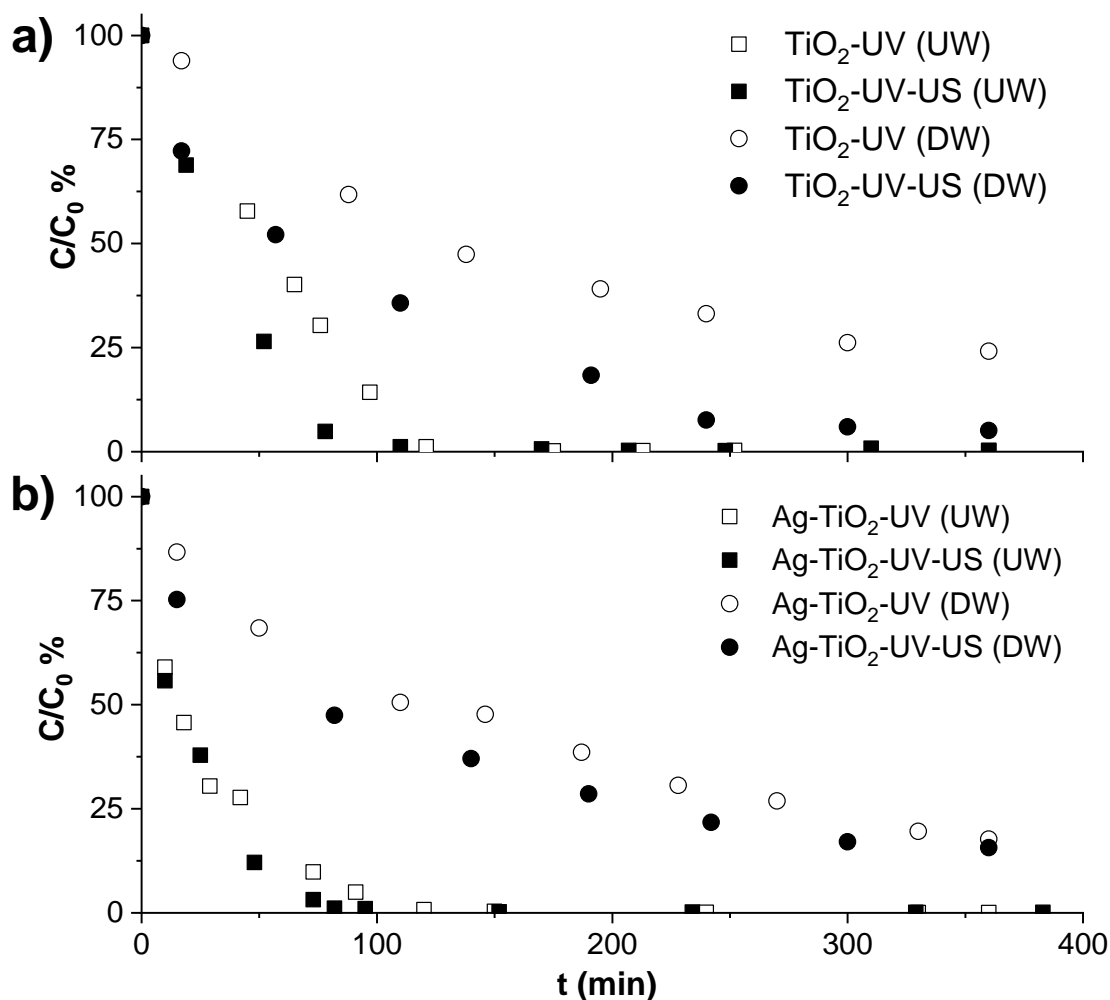


Figure 5 – Comparison of the performance of pristine TiO₂ (a) and Ag-TiO₂ (b): DC disappearance curves in photocatalytic and ultrasound-assisted photocatalytic tests in ultrapure (UW) and drinking water (DW).

The addition of Ag particles, on the one hand, promotes the DC degradation in ultrapure water, leading to a 120% and 35% increase in the DC removal rate for photocatalytic and ultrasound-assisted photocatalytic processes, respectively. On the other hand, tests in drinking water show comparable performance or even negative effects upon Ag-decoration of TiO₂. This is in good agreement with literature reports showing that electrolytes commonly present in drinking water (sulfates, carbonates and bicarbonates) can cause detrimental effects on the photocatalytic activity of Ag-decorated TiO₂ [57] [58].

Moreover, while a beneficial effect of sonication can be observed for both photocatalysts, tests with Ag-TiO₂ exhibit more limited enhancements due to the coupled process with respect to pristine TiO₂. This observation is irrespective of the adopted water matrix. As a result, lower synergy indexes are determined for ultrasound-assisted photocatalytic tests with Ag-TiO₂ (Table 2), showing

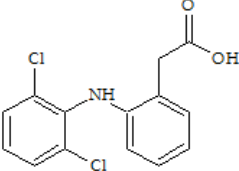
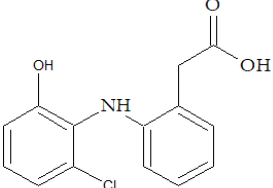
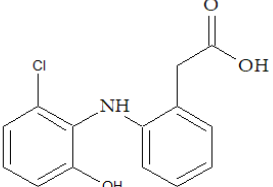
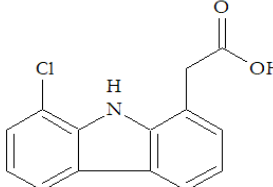
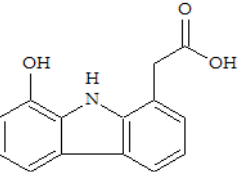
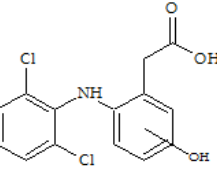
values more similar to literature reports using nano TiO₂ and conditions of high cavitation activity [16][36].

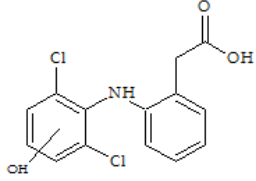
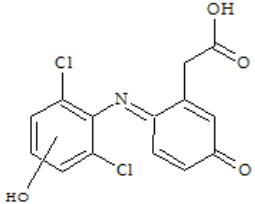
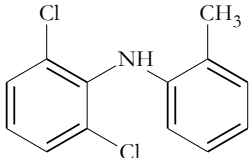
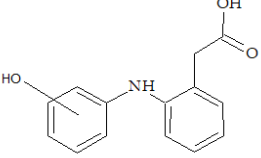
It should be noted that a role of the photocatalyst chemical nature on synergistic phenomena in sonophotochemical reactions has been previously reported: Madhavan et al. reported large differences in the synergy index of sonophotochemical DC degradation using photocatalysts of different composition [16]. In the present case, the addition of Ag seems to interfere with the mechanisms responsible for the synergistic enhancement. In this respect, TiO₂ decorated with silver-based nanoparticles can be used to produce H₂O₂ as noble metals favor the photocatalytic reduction of O₂ to H₂O₂ and Ag limits the catalytic degradation of H₂O₂ at the TiO₂ surface [59]. Hence, the addition of Ag nanoparticles could decrease the (photo)catalytic scission of H₂O₂ generated by sonication, limiting the synergistic enhancement of the combined treatment. According to this hypothesis, a similar effect should be observed also in drinking water. However, the anions present in drinking water (i.e., chlorides, bicarbonates, sulfates) could give rise to competitive adsorption at the Ag surface itself, likely erasing the beneficial effects observed using Ag-TiO₂ in ultrapure water.

3.4 Identification of Transformation Products and DC degradation pathways

The identification of possible transformation products (TPs) arising from incomplete DC degradation was carried out by UPLC/ESI-MS in negative mode. For the identification of chlorinated compounds, the characteristic isotopic pattern at M and M+2 with a 3 : 1 relative intensity was observed for analytes with one chlorine atom, whereas products containing two chlorine atoms were recognized by the characteristic isotopic pattern at M, M+2 and M+4 with relative intensities in a ratio 9 : 6 : 1. Table 3 lists the main intermediates observed during DC degradation tests by sonolysis, photocatalysis and ultrasound-assisted photocatalysis.

Table 3. Identified transformation products of diclofenac by sonolysis, photocatalysis and ultrasound-assisted photocatalysis using TiO₂ and Ag-TiO₂, along with their toxicity class according to Cramer rules with extensions [60] [61].

Product code	m/z [M-H] ⁻	Elemental composition	Proposed structure	Refs.	Toxicity class
DC	294	C ₁₄ H ₁₁ Cl ₂ NO ₂		[62]	III
TP1	276	C ₁₄ H ₁₂ ClNO ₃			III
TP1_bis	276	C ₁₄ H ₁₂ ClNO ₃		-	III
TP2	258	C ₁₄ H ₁₂ ClNO ₂		[62] [48] [63] [64] [65]	III
TP3	240	C ₁₄ H ₁₁ NO ₃		[62] [63] [65]	III
TP4	310	C ₁₄ H ₁₁ Cl ₂ NO ₃		[62] [66] [67] [68] [16] [69]	III

TP4-bis	310	$C_{14}H_{11}Cl_2NO_3$		[66] [67] [68] [16] [69] [62]	III
TP5	324	$C_{14}H_9Cl_2NO_4$		[48]	III
TP6	249	$C_{13}H_{11}Cl_2N$		[64]	III
TP7	242	$C_{14}H_{13}NO_3$		-	III
TP8	309	unknown	unknown	-	III

Most of the identified compounds are in good agreement with literature reports of DC degradation intermediates (see Table 3, column 5). Moreover, in the ultrasound-assisted tests, a few not previously reported transformation products were observed (TP7-8); for the former, the elemental composition and structure is here proposed, even though further investigations by high resolution MS analyses are needed to confirm the present hypothesis.

By analyzing the identified TPs for photocatalytic and ultrasound-assisted photocatalytic tests, the DC degradation can be proposed to proceed via the main pathways reported in Figure 6. It should be noted that our results support similar reaction pathways for photocatalytic and ultrasound-assisted photocatalytic DC degradation.

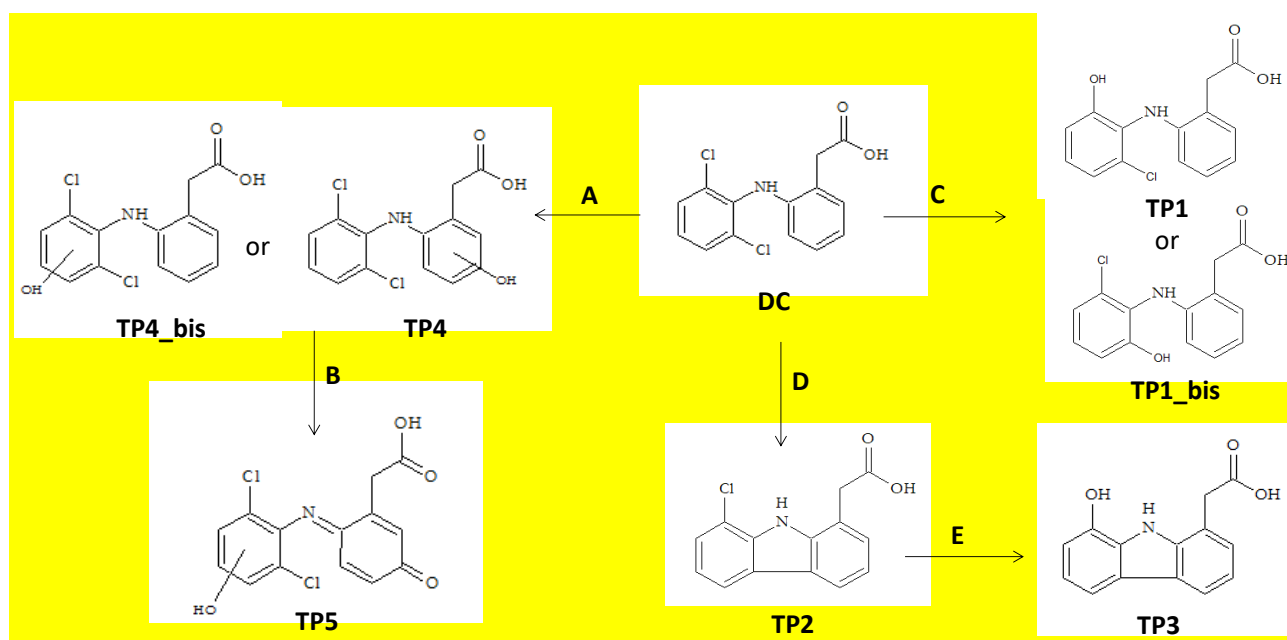


Figure 6. Proposed main pathways of DC degradation by photocatalysis and ultrasound-assisted photocatalysis.

Figure 6 shows that oxidation is one of the major degradation mechanisms, as confirmed by the identification of TP1 and TP4, and in good agreement with the literature about photocatalytic and sonolytic DC degradation [62]. In particular, hydroxyl radicals seem to play a major role, supporting the proposed mechanism of synergistic enhancement. The TP4 and TP4bis species are likely the result from the addition of $\cdot\text{OH}$ radicals to the aromatic rings (pathway A), whereas TP1 and TP1_bis can occur via the displacement of a chlorine substituent by a hydroxyl radical (pathway C). It is noteworthy that, during sonolysis experiments, the only intermediate detected in appreciable amounts was TP4, supporting a reaction mechanism driven by cavitation-generated hydroxyl radicals. On the contrary, TP4 was not appreciable during photolysis tests.

Among the other transformation products detected during photocatalytic and ultrasound-assisted photocatalytic tests, TP5 presents two hydrogen atoms less than TP4, supporting the formation of a benzoquinone imine (pathway B), in agreement with the literature [62]. The TP2 species could result from the loss of a chlorine substituent in DC, causing a cyclization reaction that leads to the formation of a carbazole ring (pathway D). The displacement of the remaining chlorine atom in the TP2 species by a hydroxyl radical can be responsible for the TP3 formation, as supported by a 18 Da mass decrease from TP2 to TP3 (pathway E). The TP6 intermediate could be obtained directly by DC via the decarboxylation [64]. The formation of TP7 can instead occur from TP1bis by loss of chlorine, analogously to photolysis mechanisms reported for DC [48].

It should be noted that all of the detected transformation compounds still belong to the high toxicity class (Table 3, column 6) estimated according to the Cramer rules with extensions. Indeed, the toxicity of initial transformation products of DC during AOPs [67] [69], like hydrodiclofenac isomers [35], has been widely reported. However, the overall toxicity of the reaction mixture decreases upon further degradation, as a result of the loss of heteroatoms from the initial chloroderivatives [69].

Most of the detected TPs showed a bell-shape trend, while in some cases a constant increase during the reaction time was observed. This is clear by considering the evolution trends of TP4 and TP1 (Figure 7).

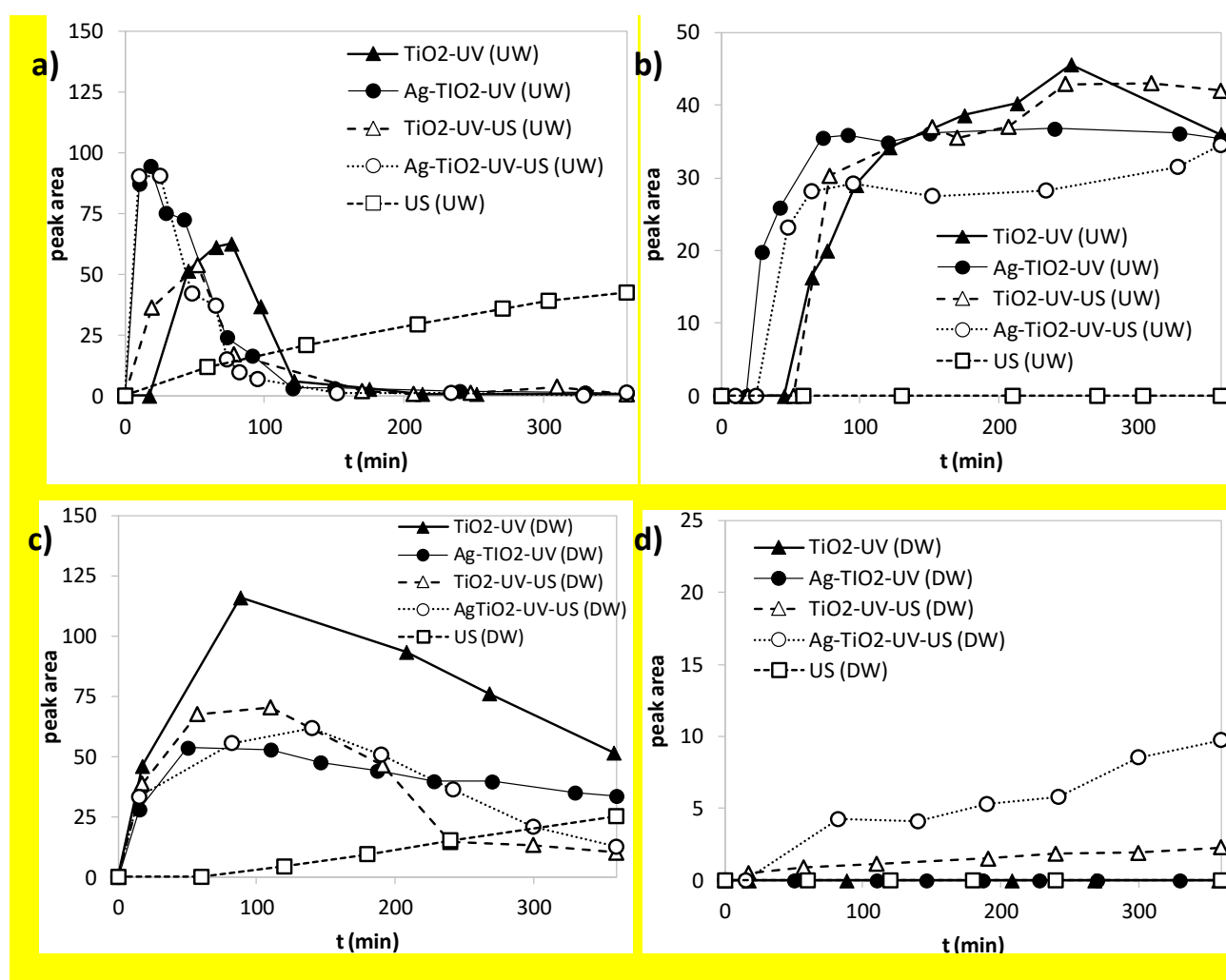


Figure 7 - Evolution trend of selected intermediates, (TP4) (a,c) and (TP1) (b,d), during sonolysis, photocatalysis and ultrasound-assisted photocatalysis tests in ultrapure water, UW (a,b) and drinking water, DW (c,d).

Figure 7a,c shows that TP4 exhibits a bell-shaped time profile in most of the photocatalytic and sonophotocatalytic tests. Only in the sonolysis tests, a constant increase is appreciable with time, which is indicative of a slower reaction kinetics, in good agreement with DC disappearance rate constants. The second considered transformation product, TP1, shows instead a constant increase in time during photocatalytic and sonophotocatalytic tests, whereas it is absent in sonolysis runs (Figure 7b,d).

By comparing panels a,b with c,d in Figure 7, the role of the water matrix can be appreciated: tests in drinking water show broader bell-shaped profiles for TP4 and a slower or absent build up of TP1, indicative of an overall slower reaction kinetics. **In this respect, it should be noted that the y-axis scale in panel b (tests in drinking water) has a maximum value of 25, which is half than the relative value in panel b (tests in ultrapure water).**

The role of the photocatalyst on the intermediate time profiles can also be discussed. Ag-promoted TiO₂ shows, in tests in ultrapure water, TP profiles indicative of a faster DC degradation with respect to pristine TiO₂ (shorter degradation time of TP4, faster build up of TP1). On the other hand, tests in drinking water exhibit no clear winner in terms of the most performing photocatalyst, with both TiO₂ and Ag-TiO₂ presenting similar TP time profiles. These observations mirror the DC removal rates discussed in Section 3.3.

Most interestingly, the effect of the combined treatment on the time profile of TPs can be appreciated in Figure 7. The TP time profiles of tests using pristine TiO₂ in ultrapure water confirm a faster DC degradation during the ultrasound-assisted photocatalytic process, especially in terms of the TP4 trend. Conversely, comparable performance are observed for photocatalytic and sonophotocatalytic tests using the Ag-decorated sample in UW. In tap water, both photocatalysts exhibit instead a clear beneficial effect of the ultrasound-assisted process with respect to the sole photocatalysis, as shown by the faster degradation of TP4 and by the clear increasing trend of TP4, the latter absent in the photocatalytic tests. These observations are also supported by the identification of numerous highly oxidized TPs (TP3, TP5, TP7, TP8) during ultrasound-assisted photocatalytic tests, which are instead barely appreciable or absent using only photocatalysis. We can thus conclude that the synergistic effects of sonophotocatalysis extends beyond the DC removal, leading to a faster degradation of prominent intermediates. Moreover, combining sonication to the photocatalytic degradation of DC is a profitable alternative whenever the photocatalysis alone is sluggish, due to the inherent activity of the photocatalyst or to demanding working conditions, like in real water matrices.

4. Conclusions

The degradation of DC by a sonophotocatalytic approach using micrometric TiO₂ and pulsed, low frequency ultrasound was here investigated. The combined method provides marked synergistic enhancements in terms of DC removal, especially when pristine TiO₂ is adopted. With respect to the literature, the present results favorably compare with previous reports both in terms of synergy index as well as of photocatalytic performance using micrometric TiO₂.

The synergism between the two combined AOPs could be related to the sonolytic formation of H₂O₂ and its subsequent scission in reactive hydroxyl radicals at the photocatalyst surface. In this respect, reaction intermediates identified by UPLC-MS analyses supported a main role of hydroxyl radicals in the sonophotocatalytic degradation pathways.

The time profiles of the main transformation products support a beneficial effect of the combined treatment also at later stages of the degradation reaction, which is a crucial aspect given the high toxicity of the initial reaction intermediates. These effects are more marked when the less performing photocatalyst (pristine TiO₂) is employed or for tests in a real water matrix.

Tests in a real-life drinking water matrix highlighted the detrimental role of ubiquitous inorganic anions on the photocatalytic and sonophotocatalytic performance. In this respect, tests in ultrapure water (the default water matrix in most literature studies) proved misleading when the actual performance in complex matrices were to be evaluated: not only the DC degradation rate varied in absolute terms but also opposite trends emerged in comparative studies between different photocatalysts, as shown by the comparison of pristine and Ag-decorated TiO₂.

Overall, the presently adopted combined approach showed promising performance and it can represent a viable strategy, in terms of energy cost and environmental impact, to conventional sonophotocatalytic setups using high frequency US and nanometric photocatalysts.

5. Acknowledgement

The Authors acknowledge Projet de cooperation Quebec Italie 2017-2019 (project number: QU17MO09) for granting the mobility of researchers between Canada and Italy. This research was undertaken, in part, thanks to funding from the Canada Research Chairs program.

References

- [1] Y. Peng, S. Hall, L. Gautam, Drugs of abuse in drinking water – a review of current detection methods, occurrence, elimination and health risks, *TrAC Trends Anal. Chem.* 85 (2016) 232–240. <https://doi.org/10.1016/j.trac.2016.09.011>.
- [2] A.B.A. Boxall, M.A. Rudd, B.W. Brooks, D.J. Caldwell, K. Choi, S. Hickmann, E. Innes, K. Ostapyk, J.P. Staveley, T. Verslycke, G.T. Ankley, K.F. Beazley, S.E. Belanger, J.P. Berninger, P. Carriquiriborde, A. Coors, P.C. DeLeo, S.D. Dyer, J.F. Ericson, F. Gagné, J.P. Giesy, T. Guoin, L. Hallstrom, M. V. Karlsson, D.G.J. Larsson, J.M. Lazorchak, F. Mastrocco, A. McLaughlin, M.E. McMaster, R.D. Meyerhoff, R. Moore, J.L. Parrott, J.R. Snape, R. Murray-Smith, M.R. Servos, P.K. Sibley, J.O. Straub, N.D. Szabo, E. Topp, G.R. Tetreault, V.L. Trudeau, G. Van Der Kraak, Pharmaceuticals and Personal Care Products in the Environment: What Are the Big Questions?, *Environ. Health Perspect.* 120 (2012) 1221–1229. <https://doi.org/10.1289/ehp.1104477>.
- [3] Y. Yang, Y.S. Ok, K.-H. Kim, E.E. Kwon, Y.F. Tsang, Occurrences and removal of pharmaceuticals and personal care products (PPCPs) in drinking water and water/sewage treatment plants: A review, *Sci. Total Environ.* 596–597 (2017) 303–320. <https://doi.org/10.1016/j.scitotenv.2017.04.102>.
- [4] R. Gothwal, T. Shashidhar, Antibiotic Pollution in the Environment: A Review, *CLEAN - Soil, Air, Water.* 43 (2015) 479–489. <https://doi.org/10.1002/clen.201300989>.
- [5] N. Le-Minh, S.J. Khan, J.E. Drewes, R.M. Stuetz, Fate of antibiotics during municipal water recycling treatment processes, *Water Res.* 44 (2010) 4295–4323. <https://doi.org/10.1016/j.watres.2010.06.020>.
- [6] A. Jia, Y. Wan, Y. Xiao, J. Hu, Occurrence and fate of quinolone and fluoroquinolone antibiotics in a municipal sewage treatment plant, *Water Res.* 46 (2012) 387–394. <https://doi.org/10.1016/j.watres.2011.10.055>.
- [7] J. Trawiński, R. Skibiński, Studies on photodegradation process of psychotropic drugs: a review, *Environ. Sci. Pollut. Res.* 24 (2017) 1152–1199. <https://doi.org/10.1007/s11356-016-7727-5>.
- [8] R. Andreozzi, M. Canterino, R. Marotta, N. Paxeus, Antibiotic removal from wastewaters: The ozonation of amoxicillin, *J. Hazard. Mater.* 122 (2005) 243–250. <https://doi.org/10.1016/j.jhazmat.2005.03.004>.
- [9] U. von Gunten, Ozonation of drinking water: Part I. Oxidation kinetics and product formation, *Water Res.* 37 (2003) 1443–1467. <https://doi.org/10.1016/S0043->

1354(02)00457-8.

- [10] E. CHAMBERLAIN, C. ADAMS, Oxidation of sulfonamides, macrolides, and carbadox with free chlorine and monochloramine, *Water Res.* 40 (2006) 2517–2526. <https://doi.org/10.1016/j.watres.2006.04.039>.
- [11] X. Chen, B. Xiao, J. Liu, T. Fang, X. Xu, Kinetics of the oxidation of MCRR by potassium permanganate, *Toxicon.* 45 (2005) 911–917. <https://doi.org/10.1016/j.toxicon.2005.02.011>.
- [12] V. Ragaini, E. Selli, C. Letizia Bianchi, C. Pirola, Sono-photocatalytic degradation of 2-chlorophenol in water: kinetic and energetic comparison with other techniques, *Ultrason. Sonochem.* 8 (2001) 251–258. [https://doi.org/10.1016/S1350-4177\(01\)00085-2](https://doi.org/10.1016/S1350-4177(01)00085-2).
- [13] R. Guan, X. Yuan, Z. Wu, L. Jiang, Y. Li, G. Zeng, Principle and application of hydrogen peroxide based advanced oxidation processes in activated sludge treatment: A review, *Chem. Eng. J.* 339 (2018) 519–530. <https://doi.org/10.1016/j.cej.2018.01.153>.
- [14] M. Salimi, A. Esrafil, M. Gholami, A. Jonidi Jafari, R. Rezaei Kalantary, M. Farzadkia, M. Kermani, H.R. Sobhi, Contaminants of emerging concern: a review of new approach in AOP technologies, *Environ. Monit. Assess.* 189 (2017) 414. <https://doi.org/10.1007/s10661-017-6097-x>.
- [15] D.B. Miklos, C. Remy, M. Jekel, K.G. Linden, J.E. Drewes, U. Hübner, Evaluation of advanced oxidation processes for water and wastewater treatment – A critical review, *Water Res.* 139 (2018) 118–131. <https://doi.org/10.1016/j.watres.2018.03.042>.
- [16] J. Madhavan, P.S.S. Kumar, S. Anandan, M. Zhou, F. Grieser, M. Ashokkumar, Ultrasound assisted photocatalytic degradation of diclofenac in an aqueous environment, *Chemosphere.* 80 (2010) 747–752. <https://doi.org/10.1016/j.chemosphere.2010.05.018>.
- [17] A. Colombo, G. Cappelletti, S. Ardizzone, I. Biraghi, C.L. Bianchi, D. Meroni, C. Pirola, F. Spadavecchia, Bisphenol A endocrine disruptor complete degradation using TiO₂ photocatalysis with ozone, *Environ. Chem. Lett.* 10 (2012) 55–60. <https://doi.org/10.1007/s10311-011-0328-0>.
- [18] Z. Khani, D. Schieppati, C.L. Bianchi, D.C. Boffito, The Sonophotocatalytic Degradation of Pharmaceuticals in Water by MnO_x-TiO₂ Systems with Tuned Band-Gaps, *Catalysts.* 9 (2019) 949. <https://doi.org/10.3390/catal9110949>.
- [19] Z. Eren, Ultrasound as a basic and auxiliary process for dye remediation: A review, *J. Environ. Manage.* 104 (2012) 127–141. <https://doi.org/10.1016/j.jenvman.2012.03.028>.
- [20] N.N. Mahamuni, Y.G. Adewuyi, Advanced oxidation processes (AOPs) involving ultrasound for waste water treatment: A review with emphasis on cost estimation, *Ultrason. Sonochem.* 17 (2010) 990–1003. <https://doi.org/10.1016/j.ultsonch.2009.09.005>.

- [21] D. Schieppati, F. Galli, M.-L. Peyot, V. Yargeau, C.L. Bianchi, D.C. Boffito, An ultrasound-assisted photocatalytic treatment to remove an herbicidal pollutant from wastewaters, *Ultrason. Sonochem.* 54 (2019) 302–310. <https://doi.org/10.1016/j.ultsonch.2019.01.027>.
- [22] J. Madhavan, F. Grieser, M. Ashokkumar, Combined advanced oxidation processes for the synergistic degradation of ibuprofen in aqueous environments, *J. Hazard. Mater.* 178 (2010) 202–208. <https://doi.org/10.1016/j.jhazmat.2010.01.064>.
- [23] C.G. Joseph, G. Li Puma, A. Bono, D. Krishnaiah, Sonophotocatalysis in advanced oxidation process: A short review, *Ultrason. Sonochem.* 16 (2009) 583–589. <https://doi.org/10.1016/j.ultsonch.2009.02.002>.
- [24] P. Wang, W. Ji, M. Li, G. Zhang, J. Wang, Bi 25 VO 40 microcube with step surface for visible light photocatalytic reduction of Cr(VI): Enhanced activity and ultrasound assisted regeneration, *Ultrason. Sonochem.* 38 (2017) 289–297. <https://doi.org/10.1016/j.ultsonch.2017.03.016>.
- [25] J. Madhavan, F. Grieser, M. Ashokkumar, Degradation of orange-G by advanced oxidation processes, *Ultrason. Sonochem.* 17 (2010) 338–343. <https://doi.org/10.1016/j.ultsonch.2009.10.008>.
- [26] J. Madhavan, F. Grieser, M. Ashokkumar, Degradation of formetanate hydrochloride by combined advanced oxidation processes, *Sep. Purif. Technol.* 73 (2010) 409–414. <https://doi.org/10.1016/j.seppur.2010.04.032>.
- [27] M. Jagannathan, F. Grieser, M. Ashokkumar, Sonophotocatalytic degradation of paracetamol using TiO₂ and Fe³⁺, *Sep. Purif. Technol.* 103 (2013) 114–118. <https://doi.org/10.1016/j.seppur.2012.10.003>.
- [28] S. Park, S. Lee, B. Kim, S. Lee, J. Lee, S. Sim, M. Gu, J. Yi, J. Lee, Toxic effects of titanium dioxide nanoparticles on microbial activity and metabolic flux, *Biotechnol. Bioprocess Eng.* 17 (2012) 276–282. <https://doi.org/10.1007/s12257-010-0251-4>.
- [29] B.J. Panessa-Warren, J.B. Warren, S.S. Wong, J.A. Misewich, Biological cellular response to carbon nanoparticle toxicity, *J. Phys. Condens. Matter.* 18 (2006) S2185–S2201. <https://doi.org/10.1088/0953-8984/18/33/S34>.
- [30] C.L. Bianchi, S. Gatto, C. Pirola, A. Naldoni, A. Di Michele, G. Cerrato, V. Crocellà, V. Capucci, Photocatalytic degradation of acetone, acetaldehyde and toluene in gas-phase: Comparison between nano and micro-sized TiO₂, *Appl. Catal. B Environ.* 146 (2014) 123–130. <https://doi.org/10.1016/j.apcatb.2013.02.047>.
- [31] S. Mozia, A.W. Morawski, The performance of a hybrid photocatalysis–MD system for the treatment of tap water contaminated with ibuprofen, *Catal. Today.* 193 (2012) 213–220.

<https://doi.org/10.1016/j.cattod.2012.03.016>.

- [32] L. Rimoldi, D. Meroni, E. Falletta, V. Pifferi, L. Falciola, G. Cappelletti, S. Ardizzone, Emerging pollutant mixture mineralization by TiO₂ photocatalysts. The role of the water medium, *Photochem. Photobiol. Sci.* 16 (2017) 60–66. <https://doi.org/10.1039/C6PP00214E>.
- [33] N. Zhang, G. Liu, H. Liu, Y. Wang, Z. He, G. Wang, Diclofenac photodegradation under simulated sunlight: Effect of different forms of nitrogen and Kinetics, *J. Hazard. Mater.* (2011). <https://doi.org/10.1016/j.jhazmat.2011.05.038>.
- [34] S. Schmidt, H. Hoffmann, L.-A. Garbe, R.J. Schneider, Liquid chromatography–tandem mass spectrometry detection of diclofenac and related compounds in water samples, *J. Chromatogr. A.* 1538 (2018) 112–116. <https://doi.org/10.1016/j.chroma.2018.01.037>.
- [35] P. Sathishkumar, R.A.A. Meena, T. Palanisami, V. Ashokkumar, T. Palvannan, F.L. Gu, Occurrence, interactive effects and ecological risk of diclofenac in environmental compartments and biota - a review, *Sci. Total Environ.* 698 (2020) 134057. <https://doi.org/10.1016/j.scitotenv.2019.134057>.
- [36] M. V. Bagal, P.R. Gogate, Degradation of diclofenac sodium using combined processes based on hydrodynamic cavitation and heterogeneous photocatalysis, *Ultrason. Sonochem.* 21 (2014) 1035–1043. <https://doi.org/10.1016/j.ultsonch.2013.10.020>.
- [37] G. Cerrato, F. Galli, D.C. Boffito, L. Operti, C.L. Bianchi, Correlation preparation parameters/activity for microTiO₂ decorated with SilverNPs for NO_x photodegradation under LED light, *Appl. Catal. B Environ.* 253 (2019) 218–225. <https://doi.org/10.1016/j.apcatb.2019.04.056>.
- [38] N.F.F. Moreira, C. Narciso-da-Rocha, M.I. Polo-López, L.M. Pastrana-Martínez, J.L. Faria, C.M. Manaia, P. Fernández-Ibáñez, O.C. Nunes, A.M.T. Silva, Solar treatment (H₂O₂, TiO₂-P25 and GO-TiO₂ photocatalysis, photo-Fenton) of organic micropollutants, human pathogen indicators, antibiotic resistant bacteria and related genes in urban wastewater, *Water Res.* 135 (2018) 195–206. <https://doi.org/10.1016/j.watres.2018.01.064>.
- [39] A. Durán, J.M. Monteagudo, I. San Martín, M. Aguirre, Decontamination of industrial cyanide-containing water in a solar CPC pilot plant, *Sol. Energy.* 84 (2010) 1193–1200. <https://doi.org/10.1016/j.solener.2010.03.025>.
- [40] F. Méndez-Arriaga, S. Esplugas, J. Giménez, Photocatalytic degradation of non-steroidal anti-inflammatory drugs with TiO₂ and simulated solar irradiation, *Water Res.* 42 (2008) 585–594. <https://doi.org/10.1016/j.watres.2007.08.002>.
- [41] W.-S. Chen, S.-C. Huang, Sonophotocatalytic degradation of dinitrotoluenes and trinitrotoluene in industrial wastewater, *Chem. Eng. J.* 172 (2011) 944–951.

<https://doi.org/10.1016/j.cej.2011.07.006>.

- [42] S. Maruvada, G.R. Harris, B.A. Herman, R.L. King, Acoustic power calibration of high-intensity focused ultrasound transducers using a radiation force technique, *J. Acoust. Soc. Am.* 121 (2007) 1434–1439. <https://doi.org/10.1121/1.2431332>.
- [43] V. Ragaini, C. Pirola, S. Borrelli, C. Ferrari, I. Longo, Simultaneous ultrasound and microwave new reactor: Detailed description and energetic considerations, *Ultrason. Sonochem.* 19 (2012) 872–876. <https://doi.org/10.1016/j.ultsonch.2011.12.008>.
- [44] P. Théron, P. Pichat, C. Guillard, C. Pétrier, T. Chopin, Degradation of phenyltrifluoromethylketone in water by separate or simultaneous use of TiO₂ photocatalysis and 30 or 515 kHz ultrasound, *Phys. Chem. Chem. Phys.* 1 (1999) 4663–4668. <https://doi.org/10.1039/a902506e>.
- [45] J. Hartmann, P. Bartels, U. Mau, M. Witter, W. v. Tümpling, J. Hofmann, E. Nietzschmann, Degradation of the drug diclofenac in water by sonolysis in presence of catalysts, *Chemosphere.* 70 (2008) 453–461. <https://doi.org/10.1016/j.chemosphere.2007.06.063>.
- [46] K.S. Suslick, *Ultrasound: Its Chemical Physical and Biological Effects*, NY, 1988.
- [47] C. Baeza, D.R.U. Knappe, Transformation kinetics of biochemically active compounds in low-pressure UV Photolysis and UV/H₂O₂ advanced oxidation processes, *Water Res.* 45 (2011) 4531–4543. <https://doi.org/10.1016/j.watres.2011.05.039>.
- [48] R. Salgado, V.J. Pereira, G. Carvalho, R. Soeiro, V. Gaffney, C. Almeida, V.V. Cardoso, E. Ferreira, M.J. Benoliel, T.A. Ternes, A. Oehmen, M.A.M. Reis, J.P. Noronha, Photodegradation kinetics and transformation products of ketoprofen, diclofenac and atenolol in pure water and treated wastewater, *J. Hazard. Mater.* 244–245 (2013) 516–527. <https://doi.org/10.1016/j.jhazmat.2012.10.039>.
- [49] F.J. Beltrán, A. Aguinaco, J.F. García-Araya, Application of Ozone Involving Advanced Oxidation Processes to Remove Some Pharmaceutical Compounds from Urban Wastewaters, *Ozone Sci. Eng.* 34 (2012) 3–15. <https://doi.org/10.1080/01919512.2012.640154>.
- [50] Y. He, N.B. Sutton, H.H.H. Rijnaarts, A.A.M. Langenhoff, Degradation of pharmaceuticals in wastewater using immobilized TiO₂ photocatalysis under simulated solar irradiation, *Appl. Catal. B Environ.* 182 (2016) 132–141. <https://doi.org/10.1016/j.apcatb.2015.09.015>.
- [51] A.R. Lado Ribeiro, N.F.F. Moreira, G. Li Puma, A.M.T. Silva, Impact of water matrix on the removal of micropollutants by advanced oxidation technologies, *Chem. Eng. J.* 363 (2019) 155–173. <https://doi.org/10.1016/j.cej.2019.01.080>.
- [52] L. Rizzo, S. Meric, M. Guida, D. Kassinos, V. Belgiorno, Heterogenous photocatalytic degradation kinetics and detoxification of an urban wastewater treatment plant effluent

- contaminated with pharmaceuticals, *Water Res.* 43 (2009) 4070–4078. <https://doi.org/10.1016/j.watres.2009.06.046>.
- [53] A. Achilleos, E. Hapeshi, N.P. Xekoukoulotakis, D. Mantzavinos, D. Fatta-Kassinos, Factors affecting diclofenac decomposition in water by UV-A/TiO₂ photocatalysis, *Chem. Eng. J.* 161 (2010) 53–59. <https://doi.org/10.1016/j.cej.2010.04.020>.
- [54] D. Darowna, S. Grondzewska, A.W. Morawski, S. Mozia, Removal of non-steroidal anti-inflammatory drugs from primary and secondary effluents in a photocatalytic membrane reactor, *J. Chem. Technol. Biotechnol.* 89 (2014) 1265–1273. <https://doi.org/10.1002/jctb.4386>.
- [55] S. Linic, P. Christopher, D.B. Ingram, Plasmonic-metal nanostructures for efficient conversion of solar to chemical energy, *Nat. Mater.* 10 (2011) 911–921. <https://doi.org/10.1038/nmat3151>.
- [56] M. Stucchi, C.L. Bianchi, C. Argirusis, V. Pifferi, B. Neppolian, G. Cerrato, D.C. Boffito, Ultrasound assisted synthesis of Ag-decorated TiO₂ active in visible light, *Ultrason. Sonochem.* 40 (2018) 282–288. <https://doi.org/10.1016/j.ultsonch.2017.07.016>.
- [57] F. ZHANG, R. JIN, J. CHEN, C. SHAO, W. GAO, L. LI, N. GUAN, High photocatalytic activity and selectivity for nitrogen in nitrate reduction on Ag/TiO catalyst with fine silver clusters, *J. Catal.* 232 (2005) 424–431. <https://doi.org/10.1016/j.jcat.2005.04.014>.
- [58] A. Sowmya, S. Meenakshi, Photocatalytic reduction of nitrate over Ag–TiO₂ in the presence of oxalic acid, *J. Water Process Eng.* 8 (2015) e23–e30. <https://doi.org/10.1016/j.jwpe.2014.11.004>.
- [59] D. Tsukamoto, A. Shiro, Y. Shiraishi, Y. Sugano, S. Ichikawa, S. Tanaka, T. Hirai, Photocatalytic H₂O₂ Production from Ethanol/O₂ System Using TiO₂ Loaded with Au–Ag Bimetallic Alloy Nanoparticles, *ACS Catal.* 2 (2012) 599–603. <https://doi.org/10.1021/cs2006873>.
- [60] G.M. Cramer, R.A. Ford, R.L. Hall, Estimation of toxic hazard—A decision tree approach, *Food Cosmet. Toxicol.* 16 (1976) 255–276. [https://doi.org/10.1016/S0015-6264\(76\)80522-6](https://doi.org/10.1016/S0015-6264(76)80522-6).
- [61] I.C. Munro, R.A. Ford, E. Kennepohl, J.G. Sprenger, Correlation of structural class with no-observed-effect levels: A proposal for establishing a threshold of concern, *Food Chem. Toxicol.* 34 (1996) 829–867. [https://doi.org/10.1016/S0278-6915\(96\)00049-X](https://doi.org/10.1016/S0278-6915(96)00049-X).
- [62] S. Murgolo, I. Moreira, C. Piccirillo, P. Castro, G. Ventrella, C. Coccozza, G. Mascolo, Photocatalytic Degradation of Diclofenac by Hydroxyapatite–TiO₂ Composite Material: Identification of Transformation Products and Assessment of Toxicity, *Materials (Basel)*. 11 (2018) 1779. <https://doi.org/10.3390/ma11091779>.

- [63] D. Kanakaraju, B.D. Glass, M. Oelgemöller, Titanium dioxide photocatalysis for pharmaceutical wastewater treatment, *Environ. Chem. Lett.* 12 (2014) 27–47. <https://doi.org/10.1007/s10311-013-0428-0>.
- [64] C. Martínez, M. Canle L., M.I. Fernández, J.A. Santaballa, J. Faria, Aqueous degradation of diclofenac by heterogeneous photocatalysis using nanostructured materials, *Appl. Catal. B Environ.* 107 (2011) 110–118. <https://doi.org/10.1016/j.apcatb.2011.07.003>.
- [65] A. Agüera, L.A. Pérez Estrada, I. Ferrer, E.M. Thurman, S. Malato, A.R. Fernández-Alba, Application of time-of-flight mass spectrometry to the analysis of phototransformation products of diclofenac in water under natural sunlight, *J. Mass Spectrom.* 40 (2005) 908–915. <https://doi.org/10.1002/jms.867>.
- [66] I.B. Ivshina, E.A. Tyumina, M. V. Kuzmina, E. V. Vikhareva, Features of diclofenac biodegradation by *Rhodococcus ruber* IEGM 346, *Sci. Rep.* 9 (2019) 9159. <https://doi.org/10.1038/s41598-019-45732-9>.
- [67] H. Yu, E. Nie, J. Xu, S. Yan, W.J. Cooper, W. Song, Degradation of Diclofenac by Advanced Oxidation and Reduction Processes: Kinetic Studies, Degradation Pathways and Toxicity Assessments, *Water Res.* 47 (2013) 1909–1918. <https://doi.org/10.1016/j.watres.2013.01.016>.
- [68] Z. Hu, X. Cai, Z. Wang, S. Li, Z. Wang, X. Xie, Construction of carbon-doped supramolecule-based g-C₃N₄/TiO₂ composites for removal of diclofenac and carbamazepine: A comparative study of operating parameters, mechanisms, degradation pathways, *J. Hazard. Mater.* 380 (2019) 120812. <https://doi.org/10.1016/j.jhazmat.2019.120812>.
- [69] P. CALZA, V. SAKKAS, C. MEDANA, C. BAIOCCHI, A. DIMOU, E. PELIZZETTI, T. ALBANIS, Photocatalytic degradation study of diclofenac over aqueous TiO₂ suspensions, *Appl. Catal. B Environ.* 67 (2006) 197–205. <https://doi.org/10.1016/j.apcatb.2006.04.021>.